Neuron

Supplemental Information

IGF-1 Receptor Differentially Regulates Spontaneous and Evoked Transmission via Mitochondria at Hippocampal Synapses

Neta Gazit, Irena Vertkin, Ilana Shapira, Martin Helm, Edden Slomowitz, Maayan Sheiba, Yael Mor, Silvio Rizzoli, and Inna Slutsky

Supplemental Information

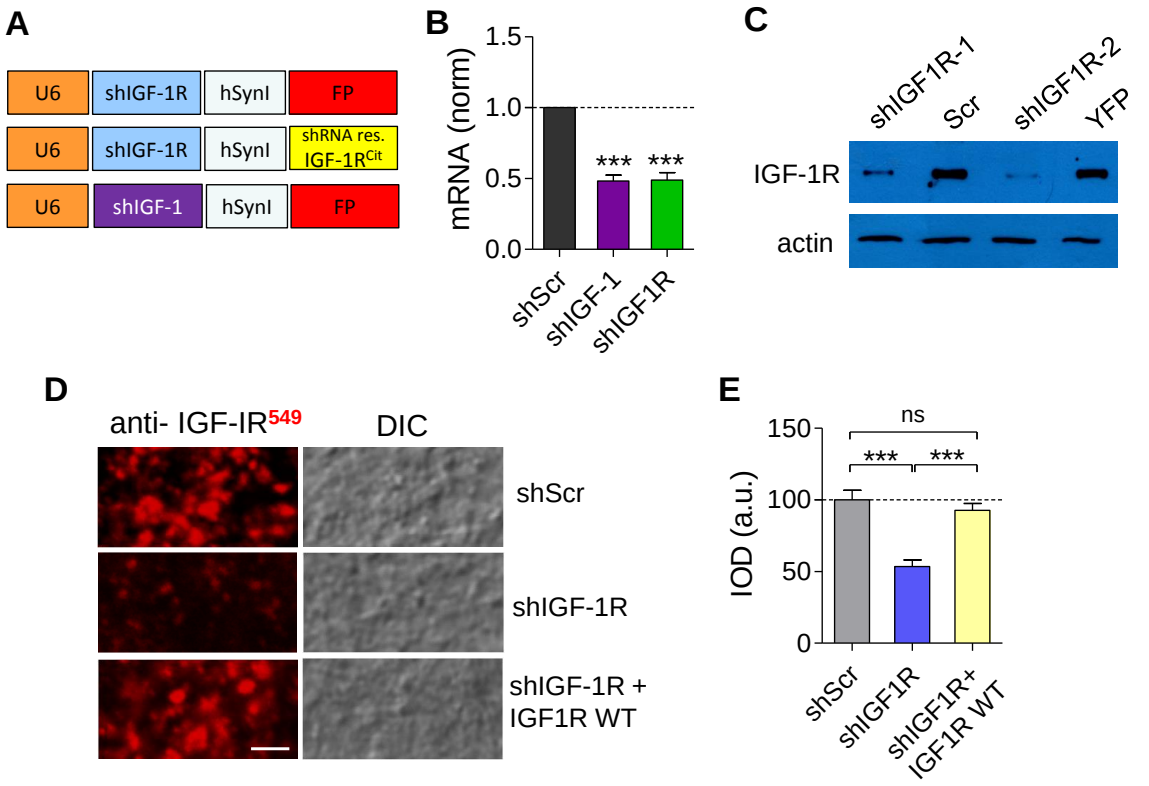

Figure S1 (related to Figures 2,3). Quantification of shRNA-dependent knockdown of IGF-1R and IGF-1

(A) Diagram of lentiviral vectors which drive expression of shRNAs for KD of IGF-1R and IGF-1 and rescue vector with shRNA-resistant hIGF-1R cDNA. U6 and SynapsinI (SynI) promoters are denoted. FP – fluorophore (mCherry for FRET experiments and GFP for FM4-64 experiments).

(B) Quantification the degree of IGF-1R and IGF-1 KD by quantitative rt-PCR (normalized to GAPDH).

(B) Western blot analysis using anti-IGF-1R antibody. Lysates of the equal amounts of primary neuronal culture infected on DIV6 by LVs encoding shRNA sequences (shIGF1R-1,2) or scrambled sequence (shScr) or eYFP. To normalize the signal, the blot was re-probed with β-Actin antibody. The shIGF1R-1 sequence was used for the experiments in Figures 2F and 3F.

(C) Representative confocal images of immunocytochemical staining of IGF-1R, demonstrating reduction in the IGF-1R expression levels following KD by shIGF1R-1 and rescue by expression of shRNA-resistant WT human IGF-1R in hippocampal cultures. Scale bar: 2 μM.

(D) IGF-1R immunocytochemical staining reveals 47 ± 5% KD following infection with shIGF-1R (n = 3) and rescue by shRNA-resistant WT IGF-1R (n = 3). ***p < 0.001 (One way ANOVA, with *post hoc* Bonferroni's Multiple Comparison Test). Data present the mean ± SEM.

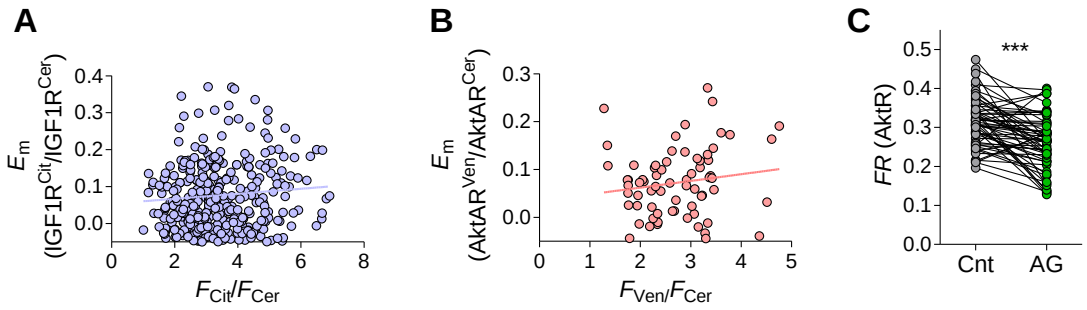

Figure S2 (related to Figure 2). Monitoring FRET at individual synapses

(A) FRET efficiency of IGF1R-Cit/Cer is plotted for individual boutons as function of intensity ratio (F_{Cit}/F_{Cer}). No correlation was found: Spearman r is 0.08 (p = 0.14).

(B) FRET efficiency of AktAR reporter is plotted for individual boutons as function of intensity ratio (F_{Van}/F_{Cer}). No correlation was found: Spearman r is 0.17 (p = 0.17).

(C) Summary of FRET ratio (*FR*) per synapse calculated by monitoring the ratio of Cit to Cer emission under Cer excitation (F_{Cit}/F_{Cer}). FRET ratio was reduced following acute application of 1 µM AG1024 (n = 60 boutons, p < 0.001).

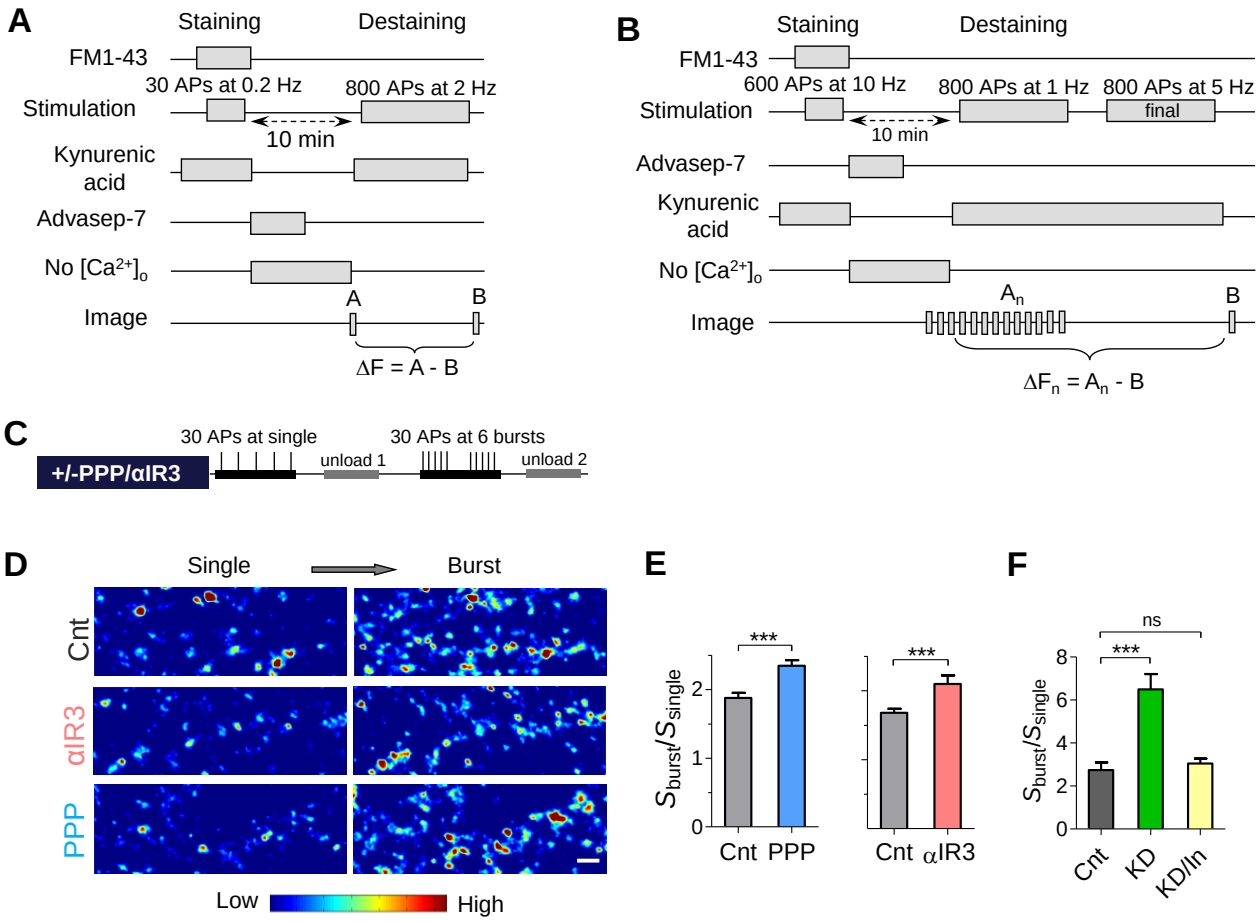

Figure S3 (related to Figures 3,5). Increased short-term synaptic facilitation following IGF-1R inhibition

(A-B) Experimental protocols to estimate synaptic vesicle recycling (A) and exocytosis (B) by FM dyes.

(C) Experimental protocol used to determine short-term plasticity (STP) indexed through STP = S_{burst}/S_{single} (S_{single}: 30 action potentials at 0.5 Hz; S_{burst}: 30 action potentials in 6 bursts, where each burst contained 5 action potentials; inter-spike interval, 10 ms; inter-burst interval, 10 s).

(D) Representative Δ*F* images for single and burst stimulations under control conditions, and following incubation with either αIR3 (4h, 1 µg/ml) or PPP (3h, 1 µM).

(E) Summary of the positive effects of PPP (*left*, n = 42 - 44) and αIR3 (*right*, n = 42 - 19) on STP.

(F) Summary of shIGF-1R (KD, n = 10), rescue experiments with shRNA-resistant IGF-1R (KD/KI, n = 15) as compared to shScr (Cnt, n = 12) cultures.

***p < 0.001 (un-paired, two-tailed *t*-test). Data present the mean ± SEM.

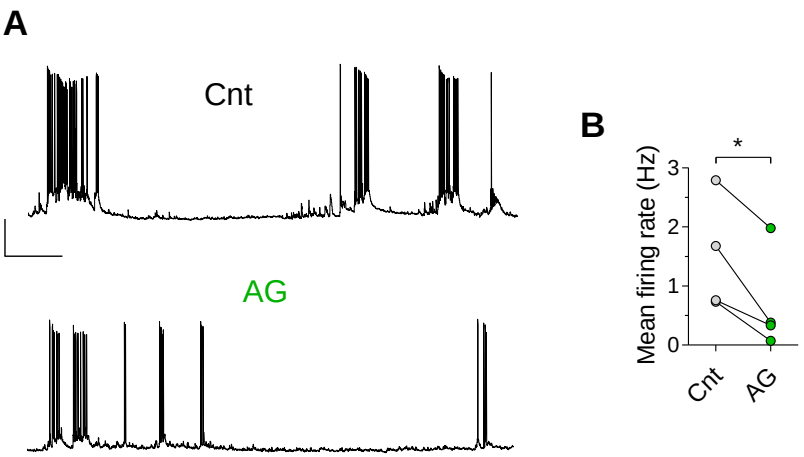

Figure S4 (related to Figure 3). IGF-1R **i**nhibition reduces spontaneous spiking rate in hippocampal neurons.

(A) Representative current clamp at resting membrane potential (-64 mV) before and 15 min after application of AG1024 (1 μM). Scale bars: 20 mV, 5 sec.

(B) Summary of the AG1024 effect on spike rate ($n = 4$, $p < 0.05$). *$p < 0.05$ (paired, two-tailed *t*-test).

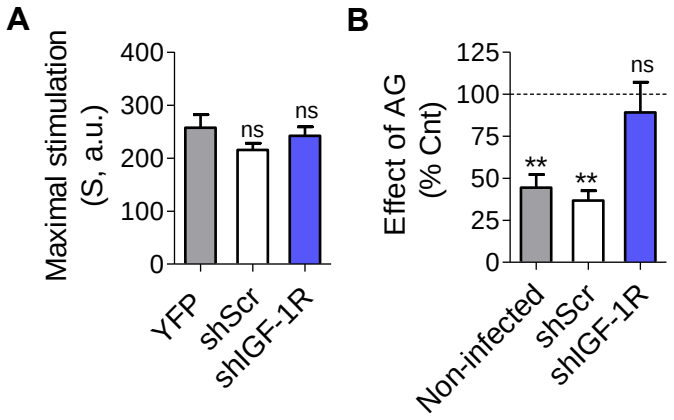

Figure S5 (related to Figure 3). Estimation of presynaptic changes following IGF-1R knockdown

(A) Quantification of total vesicle pool stained by maximal stimulation (600 APs at 20 Hz) in the presence of FM4-64. Either IGF-1R KD (n = 18) or Scr shRNA (n = 21) did not affect the amount of functional boutons in comparison to YFP only infected neurons (n = 17, $p > 0.5$).

(B) The presynaptic effect of AG1024 (1 µM, 15min) was abolished following IGF-1R KD (n = 11, $p > 0.05$), but preserved in neurons infected by Scr shRNA (n = 9, $p < 0.01$) in comparison to non-infected neurons (n = 6, $p < 0.01$). **$p < 0.01$, ns – non-significant (ANOVA analysis with *post hoc* Bonferroni's multiple comparison tests). Data present the mean ± SEM.

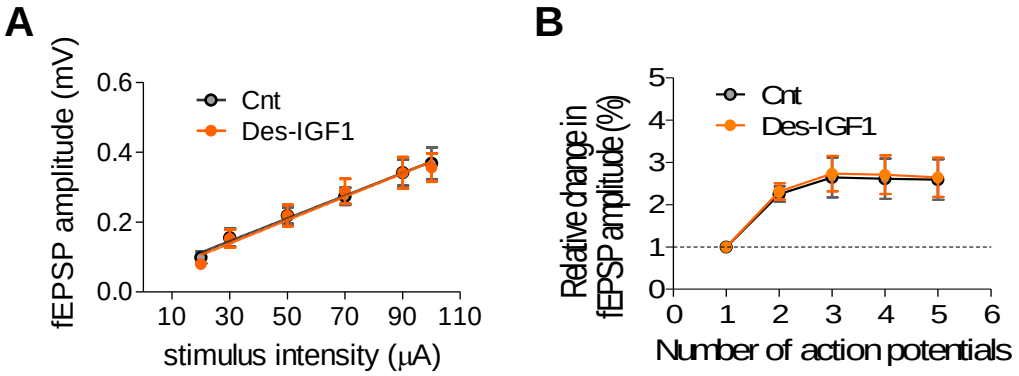

Figure S6 (related to Figure 4). Ectopic application of recombinant IGF-1 in acute slices did not affect synaptic transmission

(A) Input / output (I/O) curve calculated from fEPSP amplitude and plotted against stimulus amplitude (μA) before and 30 min after application of Des(1-3) IGF1 (50 ng/ml). There was no significant change in the slope of the I/O curve at any stimulus intensity ($n = 5$, $p > 0.5$).

(B) Peak amplitude of each fEPSP in the burst normalized to the first fEPSP amplitude, indicating short-term plasticity (STP). Application of Des(1-3)IGF1 did not change the magnitude of STP. Data present the mean ± SEM.

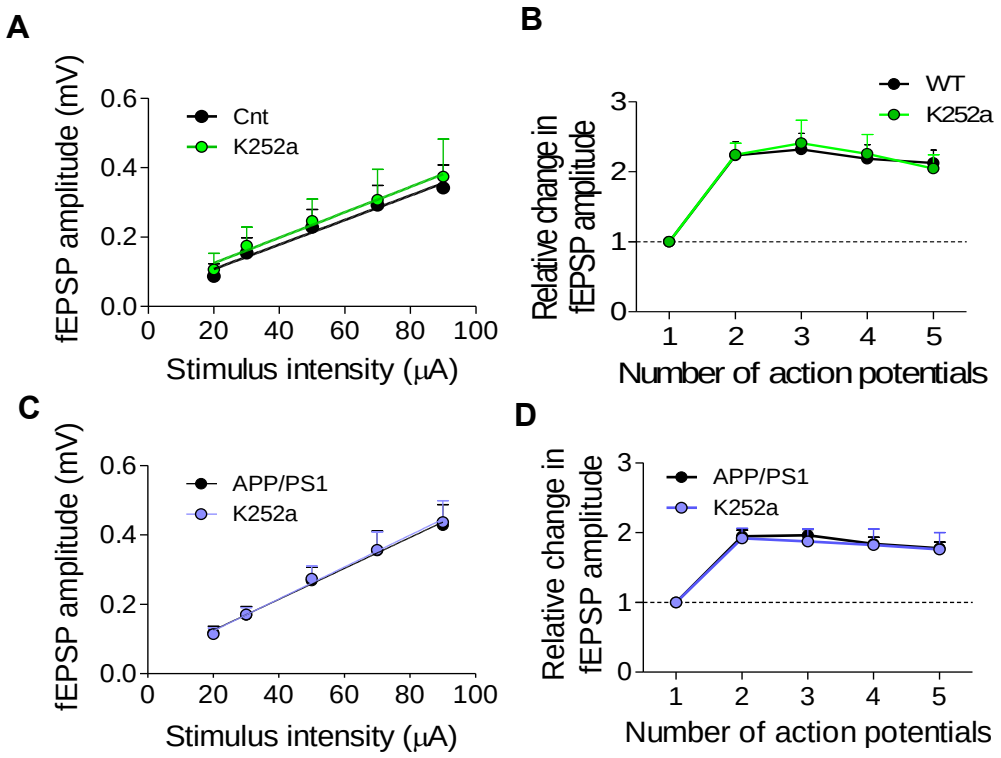

Figure S7 (related to Figure 5). Blockade of Trk receptors by K252a (200 nM) does not affect CA3-CA1 basal synaptic transmission and short-term synaptic plasticity in hippocampal slices of wild-type (A-B, n = 4, $p > 0.4$) and APP/PS1 (C-D, n = 4, $p > 0.7$) mice. Data present the mean ± s.e.m.

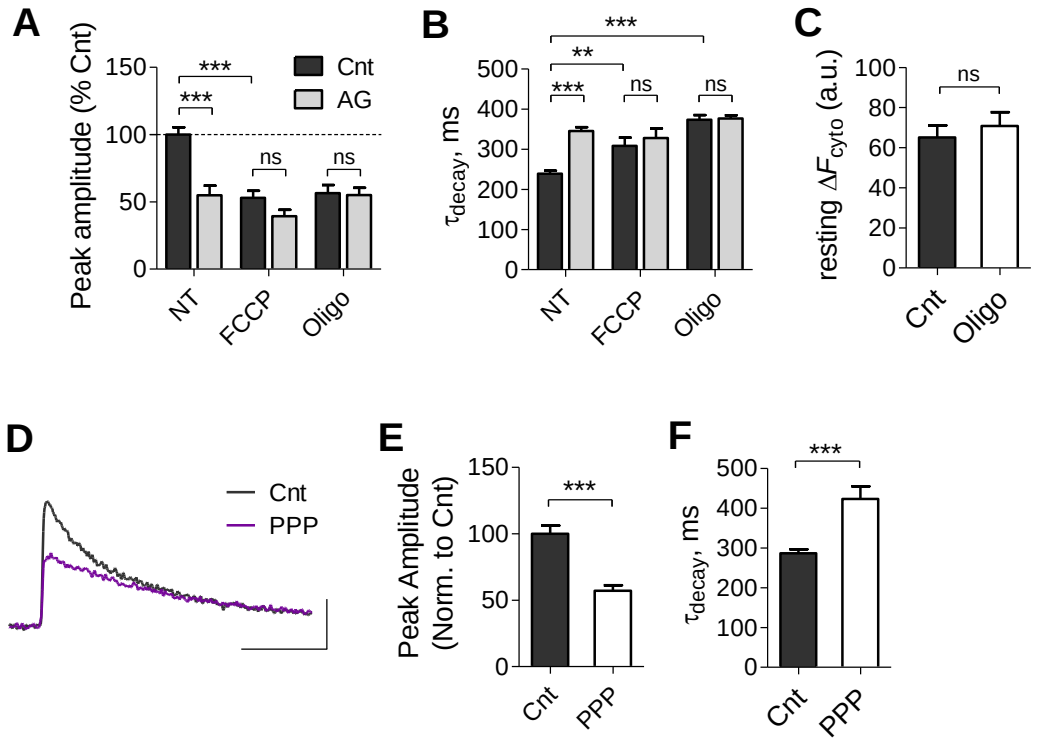

Figure S8 (related to Figure 9). Effects of AG1024 and PPP on pre-synaptic Ca^{2+} transients

(A-B) Effects of AG1024 on peak amplitude (A) and decay time-course (B) of Ca^{2+} transients in non-treated conditions (n_{cnt} =36; n_{AG} = 32), in the presence of FCCP (1 μM, n_{cnt} = 28; n_{AG} = 25) or oligomycin (1 μg/ml, n_{cnt} = 23; n_{AG} = 24). Based on the same data as Figure 9B.

(C) Oligomycin does not affect resting $[Ca^{2+}]_{cyto}$ measured by OGB-1 AM (n = 20, p = 0.39).

(D) Representative traces of Ca^{2+}_{cyto} transients evoked by 0.1 Hz stimulation during 500 Hz line scan at boutons and quantified as $\Delta F/F$ (average of 10 traces) under control conditions (n = 9) and following application (n = 13). Scale bars: 20%, 200 ms.

(E) PPP (n = 9 - 13) reduce the amplitude of Ca^{2+}_{cyto} transients.

(F) PPP increase the decay time-course of Ca^{2+}_{cyto} transients (the same experiments as in E).

**p < 0.01; ***p < 0.001. Data presented as mean ± SEM

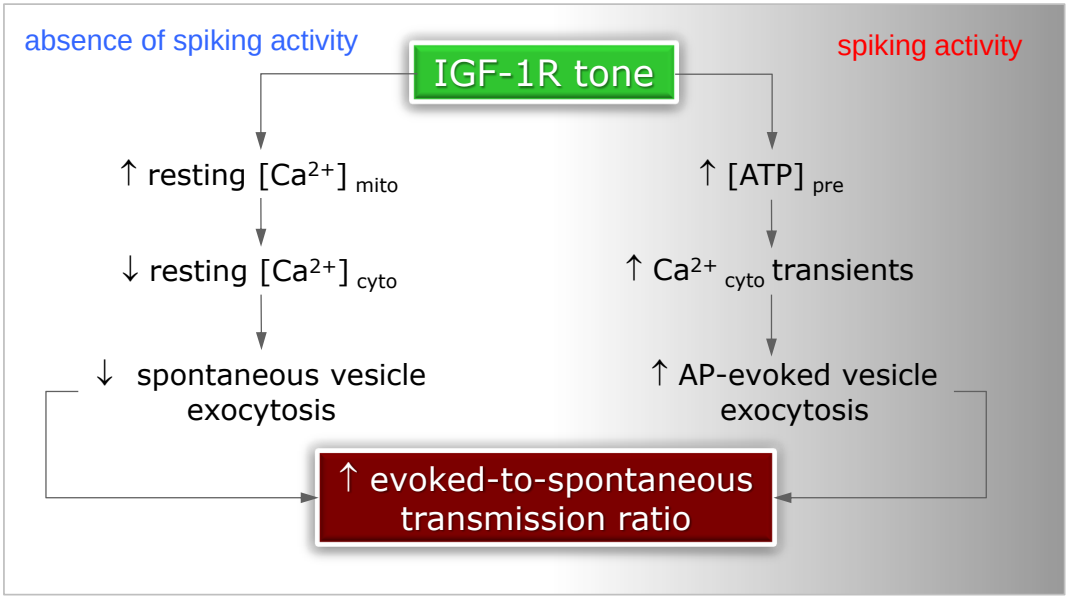

Figure S9 (related to Figure 9). Proposed model on the differential regulation of spontaneous and evoked synaptic vesicle release by IGF-1Rs

Supplemental Experimental Procedures

Primary hippocampal cultures and acute hippocampal slices. All animal experiments were approved by the Tel Aviv University Committee on Animal Care. Primary cultures of CA3-CA1 hippocampal neurons were prepared from WT mice (BALB/c background) on postnatal days 0–2, as described (Slutsky et al., 2004). Acute hippocampal slices were prepared from 2-month-old BALB/c, APPswe/PS1dE9 (Jankowsky et al., 2004) and the corresponding WT mice (B6C3F1/J background) mice. All animals were kept in a normal light/dark cycle (12h/12h), 3 animals per cage. Coronal slices (400 μm for extracellular recordings, 350 μm for intracellular patch recordings) of hippocampus were prepared as described before (Abramov et al., 2009). Slices were transferred to a submerged recovery chamber at room temperature containing oxygenated (95% O_2 and 5% CO_2) artificial cerebrospinal fluid (ACSF) for 1h before the experiment. The ACSF contained, in mM: NaCl, 125; KCl, 2.5; $CaCl_2$, 1.2; $MgCl_2$, 1.2; $NaHCO_3$, 25; NaH_2PO_4, 1.25; glucose, 25.

Plasmids, transfection, infection. AktAR FRET construct (Gao and Zhang, 2008) (Cer-FHA1-FOXO-cpVE172) was a gift of Dr. Zhang (John Hopkins University); SypI-ATeam1.03 (Shulman et al., 2015) of Dr. Daniel Gitler (Ben-Gurion University); 2mtGCamP6m of Dr. Diego De Stefani (University of Padova) and mCherry-mito of Dr. Israel Sekler (Ben-Gurion University).

Human IGF-1R was (Genbank: NM_000875) expressed in pEGFP-N1 based vector under control of CMV promoter. To construct the IGF-1R fused to mCitrine and mCerulean, cDNA of mCitrine and mCerulean were inserted between BamHI and NotI sites, while initial codon was eliminated. IGF-1R, extended by a linker PVATGS with eliminated stop codon, was inserted between NheI and BamHI sites.

For shRNA-mediated knockdown of mouse IGF-1R, we used SHCLNG-NM_010513 plasmid (Sigma-Aldrich, catalogue number TRCN0000023493**,** clone ID: NM_010513.1-3656s1c1 and TRCN0000023489, clone ID: NM_010513.1-487s1c1). The respective sequence of shRNA (according to manufacture site): CCGGCCAACGAGCAAGTTCTTCGTTCT CGAGAACGAAGAACTTGCTCGTTGGTTTTT and CCGGGCGGTGTCCAATAACT ACATTCTCGAGAATGTAGTTATTGGACACCGCTTTTT. For control of shRNA, a scrambled sequence CAGGAACGCATAGACGCATGA was cloned into the 3rd generation lentiviral plasmid pLL3.7 (Addgene #11795), using the XhoI and HpaI restriction sites, immediately following the U6 promoter.

To visualize infected cells, the sense 5' GGGCCAACGAGCAAGTTCTT CGTTCTCGAGAACGAAGAACTTGCTCGTTGGTTTTTGG and antisense 5' TCGACCAAAAACCAACGAGCAAGTTCTTCGTTCTCGAGAACGAAGAACTTGCTCGTTGGCCC oligos were annealed and cloned into pLL3.7(GFP) plasmid between HpaI and XhoI sites. The obtained plasmid was called pLL3.7-sh493. For knock-down / knock-in experiments, targeted sequence in the rescue hIGF-1R cDNA was mutated to CAAACGAACAGGTCCTCC, creating a maximum difference between the shRNAs and rescue cDNA without changing the hIGF-1R protein sequence. The cDNA encoding shRNA-resistant hIGF-1R-mCitrine was cloned between NheI and EcoRI sites of pLL3.7(GFP)-shIGF-1R plasmid.

For shRNA-mediated knockdown of mouse IGF-1, we used SHCLNG-NM_010512 plasmid (Sigma-Aldrich, catalogue number TRCN0000066354**,** clone ID: NM_010512.2-354s1c1). The sequence of shRNA (according to manufacture site):

CCGGCCCGTCCCTATCGACAAACAACTCGAGTTGTTTGTCGATAGGGACGGGTTTTTG. To visualize infected cells, the annealed oligos were re-cloned into pLL3.7(mCherry) vector (mCherry inserted between NheI and EcoRI) between HpaI and XhoI sites.

For shRNA-mediated knockdown of mouse MCU, we used SHCLNG-NM_001033259 (Sigma-Aldrich, catalogue number TRCN0000251263, clone ID: NM_001033259.3-1211s21c1). The sequence of shRNA (according to manufacture site) is: CCGGTAGGGAATAAAGGGATCTTAACTCGAGTTAAGATCCCTTTATTCCCTATTTTTG.

Transient cDNA transfections were performed using Lipofectamine-2000 reagents and neurons were typically imaged 18-24 h after transfection. Infections with LVs were done at DIV6 and the experiments were performed at >DIV14.

STED microscopy. Dual-color STED microscopy was performed as described before (Revelo et al., 2014). In brief, dissociated neuronal cultures were prepared from newborn rats and were analyzed after 9-30 days *in vitro* (Wilhelm et al., 2014). The cells were stained for IGF-1R (Cell Signaling, #3027), synaptophysin (Synaptic Systems, #101 011) and Homer1 (Synaptic Systems, #160 011), and were labeled using Chromeo494 or ATTO647N coupled secondary antibodies. Imaging was performed using a STED microscope (TCS SP5, Leica), equipped with a HCX Plan Apochromat 100x, 1.4 NA oil STED objective (Revelo et al., 2014). Data analysis was performed using a custom-written MATLAB routine (Mathworks), as follows: IGF-1R spots were selected automatically and the distance of the center-of-mass of the spot to the nearest marker spot (Synaptophysin or Homer1) was calculated. For display purposes, the images were deconvolved using the Hyugens Essential 4.4 software (Scientific Volume Imaging), as described (Revelo et al., 2014).

Confocal imaging in primary hippocampal cultures. The experiments were performed in mature (15 - 28 days *in vitro*) cultures. Hippocampal neurons were imaged using a FV1000 spectral Olympus confocal microscope using a 60 ×

1.2 NA water-immersion objective. The experiments were conducted at room temperature in extracellular Tyrode solution containing (in mM): NaCl, 145; KCl, 3; glucose, 15; HEPES, 10; $MgCl_2$, 1.2; $CaCl_2$, 1.2; pH adjusted to 7.4 with NaOH.

FM-based imaging and analysis. Activity-dependent FM1-43 and FM4-64 styryl dyes were used to estimate basal synaptic vesicle recycling and exocytosis. Action potentials were elicited by passing 50 mA constant current for 1 ms through two platinum wires, separated by ~7 mm and close to the surface of the coverslip. The extracellular medium contained 20 μM DNQX to block recurrent neuronal activity. Synaptic vesicles were loaded with 15 μM FM4-64 or 10 μM FM1-43. FM loading and unloading were done using protocols described previously (Abramov et al., 2009). The fluorescence of individual synapses was determined from the difference between images obtained after staining and after destining (ΔF). To estimate vesicle recycling / release during low frequency stimulation, we quantified: (i) ΔF signal for staining by 30 action potentials at a rate of 0.5 - 1 Hz stimulation; (ii) FM destaining rate during 1 Hz stimulation following staining of boutons by maximal stimulation. Detection of signals was done using custom-written scripts in MATLAB (Mathworks) as described before (Abramov et al., 2009).

Detecting calcium transients. For monitoring presynaptic cytosolic Ca^{2+} transients, fluorescent calcium indicator Oregon Green 488 BAPTA-1 AM (OGB-1 AM) was dissolved in DMSO to yield a concentration of 1 mM. For cell loading, cultures were incubated at 37 °C for 30 min with 3 μM of this solution diluted in Tyrode solution. For detection of Ca^{2+} transients in mitochondria, neurons were co-transfected with 2mtGCaMP6m and mCherry-mito. Imaging was performed using FV1000 Olympus confocal microscope under 488 nm (excitation) and 510 - 570 nm (emission) for OGB1-AM and 2mtGCaMP6m, and 561 nm (excitation) and HP640 nm (emission) for mCherry-mito. 500 Hz line scanning was used for OGB-1 AM; 0.3 Hz area scan was used for 2mtGCaMP6m to minimize bleaching. Data analysis was preformed using ImageJ software.

FRET imaging and analysis. Image acquisition parameters were optimized for maximal signal-to-noise ratio and minimal phototoxicity, without averaging. Images were 512 × 512 pixels, with a pixel width of 92 – 110 nm. The experiments were conducted at room temperature in Tyrode's solution. To block spikes, TTX (0.5 μM) was added to the extracellular solution. Intensity-based FRET imaging was carried as described before (Laviv et al., 2010). Briefly, the donor (Cer/mseCFP) was excited at 440 nm, and its emission was measured at 460-500 nm before (I_{DA}) and after (I_D) acceptor (Cit or cpmVen) photobleaching. Excitation was delivered to the acceptor at 514 nm, and emission was measured at 530–600 nm. Photobleaching of Cit or cpmVen was carried out with the 514 nm laser line, by a single point activation module for rapid and efficient multi-region bleaching. The FRET efficiency, E_m, was calculated thus: $E_m = (1 - I_{DA})/I_D$. Detection of signals was done using custom-written scripts in MATLAB as described earlier (Laviv et al., 2010).

Electrophysiology. Experiments in acute hippocampal slices were performed at room temperature in ACSF solution in a recording chamber on the stage of BX51WI Olympus microscope. EPSCs and fEPSPs were recorded with a glass pipette containing Tyrode solution (1 – 2 MΩ) from synapses in the CA1 stratum radiatum or synapses in stratum lacunosum moleculare using a MultiClamp700B amplifier (Molecular Devices). Stimulation of the SC pathway was delivered through a glass suction electrode (10 – 20 μm tip) filled with Tyrode. For mEPSCs recordings in hippocampal cultures, tetrodotoxin (TTX; 1 μM), amino-phosphonopentanoate (AP-5; 50 μM), and gabazine (30 μM) were added to Tyrode solution. EPSCs and mEPCSc were recorded at room temperature using the following intracellular solution (in mM): Cs-$MeSO_3$, 120; HEPES, 10; NaCl, 10; $CaCl_2$, 0.5; Mg^{2+}-ATP, 2; Na_3GTP, 0.3; EGTA, 10; pH adjusted to 7.25 with NaOH. Serial resistance was not compensated. Recordings with access resistances that exceeded 20 MΩ (for evoked EPSCs) or 10 MΩ (for mEPSCs) or that varied by >20% were excluded from analysis. Electrophysiological data were analyzed using MiniAnalysis (Synaptosoft) for mEPSCs, and in pClamp10 (Molecular Devices) for EPSCs and fEPSPs.

Lentivirus production. Recombinant lentiviruses were produced as previously described (Fogel et al., 2014). Briefly, HEK293 cells were transfected by calcium phosphate with four plasmids, the lentiviral shuttle vector, pLP/VSVG, pLP1 and pLP2. The HEK293 culture media was collected 24 and 48 h after transfection and filtered with 0.45 μm PVDF filter (Millipore) to remove cellular debris followed by centrifugation at 25,000 x RPM at 15^0C to concentrate the virus. Concentrated virus was dissolved in a small volume of PBS, aliquoted and stored frozen at -80°C.

Chemical reagents. AG1024 was purchased from Enzo Life Sciences, αIR3 was purchased from Mercury, DNQX, BAPTA-AM, thapsigargin and gabazine were purchased from Tocris; Picropodophyllin, AP-5, cadmium chloride, dantrolene, FCCP and oligomycin were purchased from Sigma; tetrodotoxin from Alomone Labs, human IGF-1 and des-(1-3)IGF-1 from Peprotech Asia, rat IGF-1 from R & D systems, αIR3 antibody from Merck Millipore (GR11), FM1-43, FM4-64 and advasep-7 from Biotium.

Quantification of shRNA-mediated knockdown efficiency. Primary neuronal cultures were infected with LV particles containing shRNAs on DIV6 and collected for RNA extraction on DIV14. RNA was immediately extracted using the RNeasy Mini kit (Qiagen Inc.) following the manufacturer's protocol. The equal amount of mRNA was reverse-transcribed to cDNA with Superscript III reverse transcriptase (Invitrogen, cat. No: 18080-051). Real-time qPCR was performed with TaqMan probes (Applied Biosystems) for IGF-1R (Mm00802831_m1), IGF-1 (Mm00439560_m1), MCU (Mm01168773_m1), GAPDH (Mm99999915_g1), the latter served as an endogenous

reference. Reactions were run in triplicate in a StepOnePlus real-time PCR system (Applied Biosystems). mRNA abundance was calculated by means of the comparative cycle threshold (Ct) method following the manufacturer's guidelines. The levels of IGF-1R, IGF-1 and MCU mRNA expression were normalized to GAPDH.

Immunocytochemistry: Cultures were fixed by 4% formaldehyde in phosphate buffer saline (PBS) solution for 20 minutes and permeabilized with 0.25% Triton X-100 for 10 minutes. Nonspecific antigens were blocked with 10% goat serum for 1 hr. Primary antibody against IGF-1R (1:500, Cell Signaling, #3027) in PBS with 5% goat serum was applied for an over-night incubation, followed by rinses in PBS and labeling with Dylight-549-conjugated secondary antibody in PBS with 2% goat serum (1:1000; Jackson ImmunoResearch Laboratories, USA) at room temperature for 1 hr. All images were collected at 1024 x 1024 pixels with a 72 nm/pixel resolution, 0.8 µm z-steps.

Statistical analysis. Error bars shown in the figures represent standard error of the mean (s.e.m.). For biochemical and electrophysiological experiments, n is designated for the number of animals. For imaging experiments, n is designated for the number of synapses (each experimental condition was repeated at least in 3 different batches of cultures). One-way ANOVA analysis with *post hoc* Bonferroni's were used to compare several conditions. Two-way ANOVA with *post hoc* Bonferroni's were used to compare short-term synaptic plasticity during burst of 5 stimuli under different conditions. Unpaired two-tailed *t*-tests were used for two-group comparison. Nonparametric Spearman test has been used for correlation analysis. $*p < 0.05$; $**p < 0.01$; $***p < 0.001$.

Supplemental References:

Abramov, E., Dolev, I., Fogel, H., Ciccotosto, G.D., Ruff, E., and Slutsky, I. (2009). Amyloid-[beta] as a positive endogenous regulator of release probability at hippocampal synapses. Nat Neurosci 12, 1567-1576.

Fogel, H., Frere, S., Segev, O., Bharill, S., Shapira, I., Gazit, N., O'Malley, T., Slomowitz, E., Berdichevsky, Y., Walsh, Dominic M., *et al.* (2014). APP Homodimers Transduce an Amyloid-β-Mediated Increase in Release Probability at Excitatory Synapses. Cell Reports 7, 1560-1576.

Gao, X., and Zhang, J. (2008). Spatiotemporal analysis of differential Akt regulation in plasma membrane microdomains. Molecular biology of the cell 19, 4366-4373.

Jankowsky, J.L., Fadale, D.J., Anderson, J., Xu, G.M., Gonzales, V., Jenkins, N.A., Copeland, N.G., Lee, M.K., Younkin, L.H., Wagner, S.L., *et al.* (2004). Mutant presenilins specifically elevate the levels of the 42 residue beta-amyloid peptide in vivo: evidence for augmentation of a 42-specific gamma secretase. Human Molecular Genetics 13, 159-170.

Laviv, T., Riven, I., Dolev, I., Vertkin, I., Balana, B., Slesinger, P.A., and Slutsky, I. (2010). Basal GABA Regulates GABA(B)R Conformation and Release Probability at Single Hippocampal Synapses. Neuron 67, 253-267.

Revelo, N.H., Kamin, D., Truckenbrodt, S., Wong, A.B., Reuter-Jessen, K., Reisinger, E., Moser, T., and Rizzoli, S.O. (2014). A new probe for super-resolution imaging of membranes elucidates trafficking pathways. J Cell Biol 205, 591-606.

Shulman, Y., Stavsky, A., Fedorova, T., Mikulincer, D., Atias, M., Radinsky, I., Kahn, J., Slutsky, I., and Gitler, D. (2015). ATP binding to synaspsin IIa regulates usage and clustering of vesicles in terminals of hippocampal neurons. J Neurosci 35, 985-998.

Slutsky, I., Sadeghpour, S., Li, B., and Liu, G. (2004). Enhancement of synaptic plasticity through chronically reduced Ca2+ flux during uncorrelated activity. Neuron 44, 835-849.

Wilhelm, B.G., Mandad, S., Truckenbrodt, S., Krohnert, K., Schafer, C., Rammner, B., Koo, S.J., Classen, G.A., Krauss, M., Haucke, V., *et al.* (2014). Composition of isolated synaptic boutons reveals the amounts of vesicle trafficking proteins. Science 344, 1023-1028.